Journal of Cleaner Production 267 (2020) 122049

Contents lists available at ScienceDirect

Journal of Cleaner Production

journal homepage: www.elsevier.com/locate/jclepro

Spatio-temporal distribution and influencing factors of atmospheric polycyclic aromatic hydrocarbons in the Yangtze River Delta

Baojie Li [a, b], Shenglu Zhou [b, *], Teng Wang [c], Yujie Zhou [b], Liang Ge [b], Hong Liao [a, **]

[a] Jiangsu Key Laboratory of Atmospheric Environment Monitoring and Pollution Control, Collaborative Innovation Center of Atmospheric Environment and Equipment Technology, School of Environmental Science and Engineering, Nanjing University of Information Science and Technology, Nanjing, 210044, China

[b] School of Geography and Ocean Science, Nanjing University, Nanjing, 210023, China

[c] College of Oceanography, Hohai University, Nanjing, 210098, China

ARTICLE INFO

Article history:
Received 9 December 2019
Received in revised form
24 April 2020
Accepted 2 May 2020
Available online 13 May 2020

Handling editor: Prof. Jiri Jaromir Klemeš

Keywords:
Atmospheric polycyclic aromatic hydrocarbons
Source identification
Backward trajectory
Yangtze river delta

ABSTRACT

In this study, we collected samples of atmospheric polycyclic aromatic hydrocarbons (PAHs) in the Yangtze River Delta (YRD), one of the most developed regions in China, during four seasons, from June 2017 to May 2018. We identified the spatiotemporal distribution of PAHs in YRD, and analyzed the factors (source contribution, meteorological conditions, and backward trajectory) influencing these concentrations. First, our results showed that the average PAH concentration was 41.46 ± 15.57 ng/m^3 in YRD, and was highest in Jiangsu (44.47 ± 11.37 ng/m^3). The concentration of PAHs has decreased since 2001. The relatively balanced development of urban and rural areas in the YRD has resulted in a relatively low ratio (~1.12) of PAHs between urban and rural areas. The PAH level in YRD was highest in winter (52.21 ± 14.70 ng/m^3) and lowest in summer (31.23 ± 12.88 ng/m^3). Second, principal component and multivariate linear regression analyses (PCA-MLR) were used to identify three main PAH sources: vehicle emissions (52.83%), coke ovens and volatilization (23.67%), and coal and biomass combustion (23.51%). The seasonal variations in the PAH source contribution were mainly attributed to seasonal differences in the amounts of coal and biomass burned, the prevailing wind direction, and traffic control in winter. Third, we found that the PAH concentrations were significantly negatively correlated with the temperature, precipitation, and relative humidity throughout the year. Finally, backward trajectory analysis indicated that the PAHs in YRD were significantly affected by air masses from northern China, particularly during winter. The results of this study suggest that enforcing stricter controls on coal and biomass combustion in northern China, improving the fuel quality of vehicles, increasing the proportion of gas/electric vehicles, and strengthening the joint control of air pollution could further reduce the PAH concentrations in China. The analysis conducted in this study will help develop pollution control strategies to reduce lung cancer risk for the whole YRD region.

1. Introduction

Airborne polycyclic aromatic hydrocarbons (PAHs) are typically generated by incomplete combustion or pyrolysis of fossil and biomass fuels and various industrial processes (Chang et al., 2006) and exert adverse effects on human health. Atmospheric PAHs can cause lung cancer and other diseases through a variety of exposure pathways (e.g., respiration). Since China's reform and opening up in 1978, energy consumption has increased from 0.57 to 4.36 Gtce as a result of the rapid social and economic development. Large amounts of PAHs were discharged into the air, with an emission of 106 Gg, ranking first in the world (Shen et al., 2013). (Xu et al., 2018) found that the cumulative nonoccupational excess lung cancer cases associated with only benzo[a]pyrene from beehive coke ovens was 3500 (±1500) from 1982 to 2015. PAH pollution in China therefore seriously threatens ecological environment and human health.

* Corresponding author. School of Geography and Ocean Science, Nanjing University, Nanjing, 210023, China.

** Corresponding author. School of Environmental Science and Engineering, Nanjing University of Information Science and Technology, Nanjing, 210044, China.

E-mail addresses: baojieli@nuist.edu.cn (B. Li), zhousl@nju.edu.cn (S. Zhou), tengwang@hhu.edu.cn (T. Wang), dg1827052@smail.nju.edu.cn (Y. Zhou), mg1727004@smail.nju.edu.cn (L. Ge), hongliao@nuist.edu.cn (H. Liao).

https://doi.org/10.1016/j.jclepro.2020.122049
0959-6526/

With the development of PAH monitoring technology over the past 20 years, PAHs have attracted worldwide attention (Hong et al., 2016). Many institutions (e.g., the Chinese Academy of Sciences, Peking University, and the Harbin Institute of Technology) have studied pollution levels and source identification of atmospheric PAHs in China. The average atmospheric PAH concentrations in China are higher than those in other countries in Asia and some developed countries (Hong et al., 2016). Many studies showed that the atmospheric PAH concentrations in China are higher in cities than in rural areas (Liu et al., 2008), and higher in northern than in southern China (Zhang et al., 2016). For example, Ma et al. (2018) observed average PAH concentrations of 239 and 165 ng/m^3, in northern and southern cities, respectively.

The atmospheric PAH concentration is mainly determined by emission sources and meteorological influences. Many studies have analyzed the PAH sources in certain regions/cities in China, and found that these differ significantly between northern and southern China. In northern China, coal and biomass burning is the predominant PAH source, especially in the cold season (Shen et al., 2019), accounting for high proportions of 78.7% (2012–2013) in Beijing (Lin et al., 2015), 59.9% (2013) in Xi'an, and 55.5% (2014–2015) in Taiyuan (Yan et al., 2017). Owing to the differences in the energy structure and high temperature, the contribution of coal and biomass burning in southern China to atmospheric PAH was found to be lower than that in northern China. Traffic was considered to be the major PAH source in the southern cities of China, with contributions of 69% (2001–2012) in Guangzhou (Li et al., 2006), and 31–43% (2012–2013) in Shanghai (Liu et al., 2017). Coal and biomass burning also significantly contributed to atmospheric PAHs in some regions of southern China due to the long-range transport of polluted air mass from northern China (Ma et al., 2016). In terms of meteorological influences, significant correlations were observed between the concentration of PAHs and precipitation (Li et al., 2016a), temperature (Wang et al., 2019), wind speed (Tan et al., 2006), and relative humidity (Hien et al., 2007). However, some studies also found that the concentration of PAHs showed no relationship with wind speed (Li et al., 2016b) and relative humidity (He et al., 2014).

To cope with heavy haze pollution, China has issued many national policies and regulations (e.g., the Air Pollution Prevention and Control Action Plan), which have effectively curbed air pollution, e.g., fine particulate matter ($PM_{2.5}$) has decreased by 30–40% across China since 2013 (Li et al., 2019). However, the pollution level and long-term trends of atmospheric PAH concentrations have been little investigated in the Yangtze River Delta (YRD) despite the relatively high toxicity of PAHs. The YRD is one of the most developed regions in China and is characterized by a high population density and well-developed industries (Zheng et al., 2016). This region accounts for less than 1% of China's area but represents 16.2% of its gross domestic product and 7.58% of its total population in 2017 (NBSC, 2018a). Moreover, rapid industrialization and urbanization have led to a 7.3-fold increase in energy consumption over the past 30 years (Li et al., 2018), which caused widespread atmospheric PAH pollution.

To date, the PAH concentrations in the YRD have only been explored in a few cities, such as Nanjing (He et al., 2014) and Shanghai (Liu et al., 2018); thus, the PAH levels between studies cannot be compared, and it is difficult to determine the spatial variation of PAHs in the YRD. More information regarding the spatiotemporal distribution of PAH concentrations in the YRD is required. Furthermore, few studies have considered the spatio-temporal distribution and influencing factors, including the source contribution, meteorological conditions, and backward trajectories. A better understanding of the spatio-temporal distribution and factors influencing the ambient PAHs throughout the YRD region will aid in the development of control strategies to reduce lung cancer risk.

Therefore, the main objectives of this study were to identify the spatio-temporal distribution of and long-term trend in atmospheric PAH concentrations in the YRD and to analyze factors (source contribution, meteorological conditions, and backward trajectory) influencing these concentrations using principal component analysis and multivariate linear regression (PCA-MLR), correlation analyses, and the Hybrid Single-Particle Lagrangian Integrated Trajectory (HYSPLIT) model.

2. Materials and methods

A wide array of PAH compounds are present in the environment. Based on their persistence, high toxicity and carcinogenic potential, 16 PAHs have been listed as "priority pollutants" by the United States Environmental Protection Agency (Keith, 2015). The 16 priority PAHs has been widely adopted by most scientists and have clear sampling and measurement methods (Andersson and Achten, 2015). So, we investigated the 16 PAHs in this study: naphthalene (NAP), acenaphthylene (ACY), acenaphthene (ACE), fluorene (FLO), phenanthrene (PHE), anthracene (ANT), fluoranthene (FLA), pyrene (PYR), benz(a)anthracene (BaA), chrysene (CHR), benzo(b)fluoranthene (BbF), benzo(k)fluoranthene (BkF), benzo(a)pyrene (BaP), dibenz(a,h)anthracene (DahA), indeno(l,2,3-cd)pyrene (IcdP), and benzo(g,h,i)perylene (BghiP). BaA, CHR, BbF, BkF, BaP, DahA, IcdP, and BghiP are carcinogenic PAHs (Carc-PAHs).

2.1. Study area and sampling

The area of the YRD investigated in this study consists of Shanghai, Southern Jiangsu (Nanjing, Wuxi, Changzhou, Suzhou, Nantong, Yangzhou, and Taizhou), and Northern Zhejiang (Hangzhou, Jiaxing, Huzhou, Shaoxing, and Zhoushan) (Fig. 1). It encompasses a total area of 9.39×10^4 km^2, accounting for less than 1% of China's area, and has a subtropical monsoon climate. The YRD is one of the world's largest urban agglomerations, with a high population density and economic development level. In 2017, the YRD accounted for 7.58 and 16.20% of China's population and gross domestic product, respectively (NBSC, 2018a). The emission density of PAHs in the YRD is higher than the national average and that of other developed regions in China (such as Pearl River Delta) (Lang et al., 2008). The YRD has a well-developed transportation network and heavy industry, and is close to the North China Plain, where the PAH pollution is severe. Therefore, the sources of PAHs in this region are relatively complex. Some studies observed significant atmospheric PAH pollution in the YRD (He et al., 2014), with the high population density further increasing the risk of lung cancer in this region.

A total of 27 sampling stations were distributed in the YRD, and the sampling period lasted from June 10, 2017 to June 14, 2018. Six sampling stations were located in rural areas and the remaining 21 were located in cities. The sampling stations covered all prefecture-level cities in the YRD (Fig. 1). There were no obvious sources of PAHs (e.g., factories or roads) around the stations, thus reducing the impact of point source pollution on PAH concentrations. The sampling period was divided into four seasons: summer (June 10 to September 4, 2017), autumn (September 4 to December 4, 2017), winter (December 4, 2017 to March 7, 2018), and spring (March 7 to June 11, 2018) (Table S1). The average sampling period was 90 days.

We used passive air samplers with polyurethane foam (PUF) disks to collect the PAHs. Such air samples have been tested extensively, and this technique has been used to effectively measure atmospheric PAHs (Hong et al., 2016). The diameter, thickness, superficial area, volume, and density of the PUF (Tisch

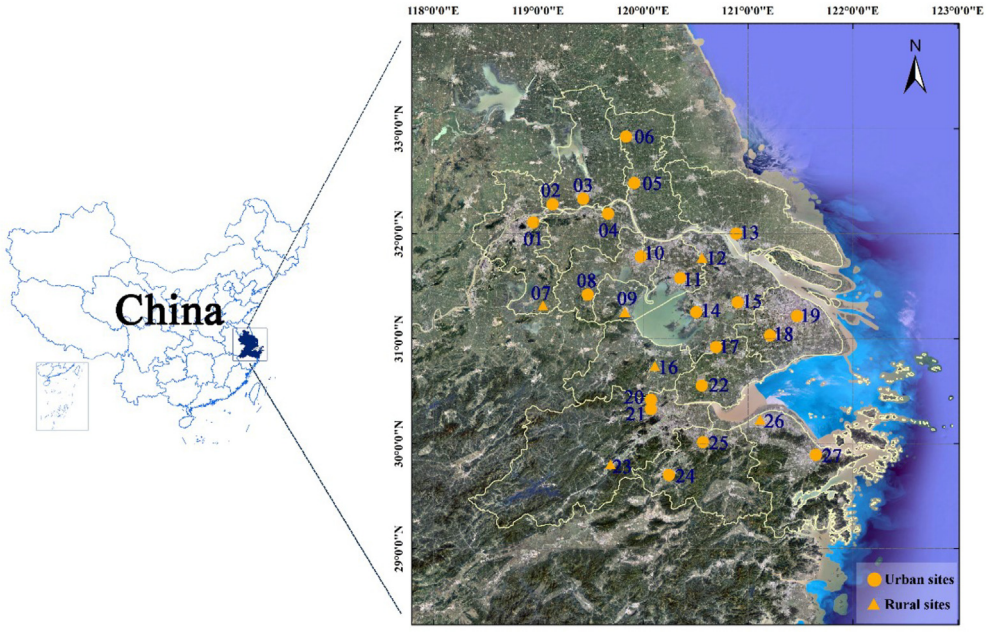

Fig. 1. Location of sampling sites in the Yangtze River Delta, China.

Environment, USA) disks were 13.97 cm, 1.27 cm, 362.29 cm^2, 194.66 cm^3, and 0.0246 g/cm^3, respectively. Prior to field sampling, the PUF disks were Soxhlet-extracted for 24 h with a 1:1 mixture of n-hexane and acetone for clean the PUF. The height of the samplers was set at 1.5 m, and those of some samplers differed slightly but never exceeded 10 m. After three months of atmospheric PAH collection (corresponding to one sampling period), the PUF disks were sent back to Nanjing University within two days after sampling, stored in sealed plastic bags at −20 °C for further analysis, and replaced with new PUF disks. After the completion of a sampling period, the samplers were cleaned prior to the installation of new PUF disks for the next sampling period. Unfortunately, one PUF disk (at site #10) in the fourth sampling period was lost.

2.2. Analysis methods

After sampling, the samples were spiked with surrogate recovery standards (D8-napthalene, D10-Acenaphthene, D10-Phenanthrene, D12-Chrysene, and D12-Perylene). The PUF disks were then extracted for 24 h with dichloromethane, using a Soxhlet extractor, and the extracts were concentrated to 2 mL, using rotary vacuum evaporation, and changed to hexane. The concentrated extracts were cleaned up using silica gel column chromatography (with an internal diameter of 25 × 1 cm, 6 g silica gel at the bottom, and 2.5 g anhydrous sodium sulfate at the top). After adding the sample extract, the column was eluted with 25 mL n-hexane followed by 50 mL n-hexane/dichloromethane (v/v = 1:1). Subsequently, the collected PAHs were vacuum-evaporated, solvent-exchanged to n-hexane, concentrated to 1 mL under a gentle nitrogen flow, and stored in gas chromatography vials for analysis.

The concentrations of the 16 studied PAHs were measured using a Shimadzu QP2010 Ultra gas chromatographer−mass spectrometer (Kyoto, Japan) equipped with a fused silica capillary column (Rtx-5MS, 0.25 mm i.d. × 30 m, with a film thickness of 0.25 μm). The carrier gas was helium at a constant flow rate of 1.0 mL/min. The gas chromatography temperature program was as follows: initial temperature of 80 °C (2 min), 80−180 °C at 20 °C/min, 180 °C (5 min), 180−290 °C at 10 °C/min, and 290 °C (15 min). The injection port was set at 290 °C. The interface and ion source were maintained at 280 and 230 °C, respectively. Ionization was carried out using the electron impact mode, and data were acquired using the selective ion monitoring mode. The PAH concentrations (ng/day) of each sample were converted to nanograms per cubic meter (ng/m^3), which was mainly determined according to the sampling days and efficiency (detailed in the Section S1). In addition, the quality assurance/quality control was detailed in Section S2.

2.3. Analysis of factors influencing atmospheric PAHs

2.3.1. Source identification using principal component analysis and multivariate linear regression

PCA-MLR is a receptor model which assumes that species with similar variability are grouped together in the lowest number of factors explaining the variability of the whole dataset, where each factor is associated with a source or source type (Larsen and Baker, 2003). PCA-MLR is a widely used model and can identify a small number of independent primary components to measure the variance in a PAHs dataset (Zhang et al., 2019a).

In this study, the PCA-MLR model was run using SPSS 21. First, PCA was conducted to identify the PAH sources. The factor loading and score matrices can be calculated by using the following equation:

$$Y = X \times L \quad (1)$$

where Y is the normalized concentration matrix for the 16 PAHs, X is the factor score matrix, and L is the factor loading matrix. Before statistical analysis, the raw PAH concentration matrix was standardized using the Z-score to assign equal weighting to each variable in the PCA. The principal components (PCs) were rotated using the varimax rotation method, and those with an eigenvalue of >1 were retained.

MLR was then applied to quantify the identified source contributions of atmospheric PAHs, with the PCA factor scores (X) and normalized total PAH concentrations as the independent and dependent variables, respectively (Larsen and Baker, 2003). The basic equation of a multiple linear model is as follows:

$$Z = \sum B_i \times X_i \quad (2)$$

where Z is the standardized normal deviates of $\sum$PAHs, X_i is the factor score matrix, and B_i is the MLR regression coefficient. The contribution of source k can be obtained by equation (3):

$$k(\%) = B_k \Big/ \sum B_i \quad (3)$$

2.3.2. Impact of meteorological conditions

Precipitation, temperature, relative humidity, and wind speed were used to study the effects of meteorological conditions on the concentrations of atmospheric PAHs. Daily meteorological data were obtained from the European Center for Medium-Range Weather Forecasts Era-Interim Reanalysis Dataset (ECMWF, 2009) and interpolated to 0.25 × 0.25°. The height at which temperature and wind speed were obtained was 1.5 m, which is consistent with the installation height of the sampling stations. Fig. 2 shows the average precipitation, temperature, wind speed and relative humidity for the four sampling periods in the YRD region. To determine the influence of meteorological conditions on atmospheric PAHs in each grid in the four sampling periods, correlations between these variables were evaluated using Spearman's correlation coefficient.

2.3.3. Backward trajectory analysis

The backward trajectories were calculated using the HYSPLIT model with the National Centers for Environmental Prediction/National Center for Atmospheric Research (NCEP/NCAR) reanalysis data (Neroda et al., 2020). We used a 0.5° Global Data Assimilation System model provided by the National Weather Service's National Center for Environmental Prediction. We calculated the backward trajectories of the HYSPLIT model every day at 6 h intervals (0:00, 6:00, 12:00, and 18:00 UTC). The duration of the calculation was 48 h, and the height above the ground was 500 m, based on previous studies (Liu et al., 2018). Trajectories for each season were clustered based on the change or turning point in total spatial variance during the cluster analysis.

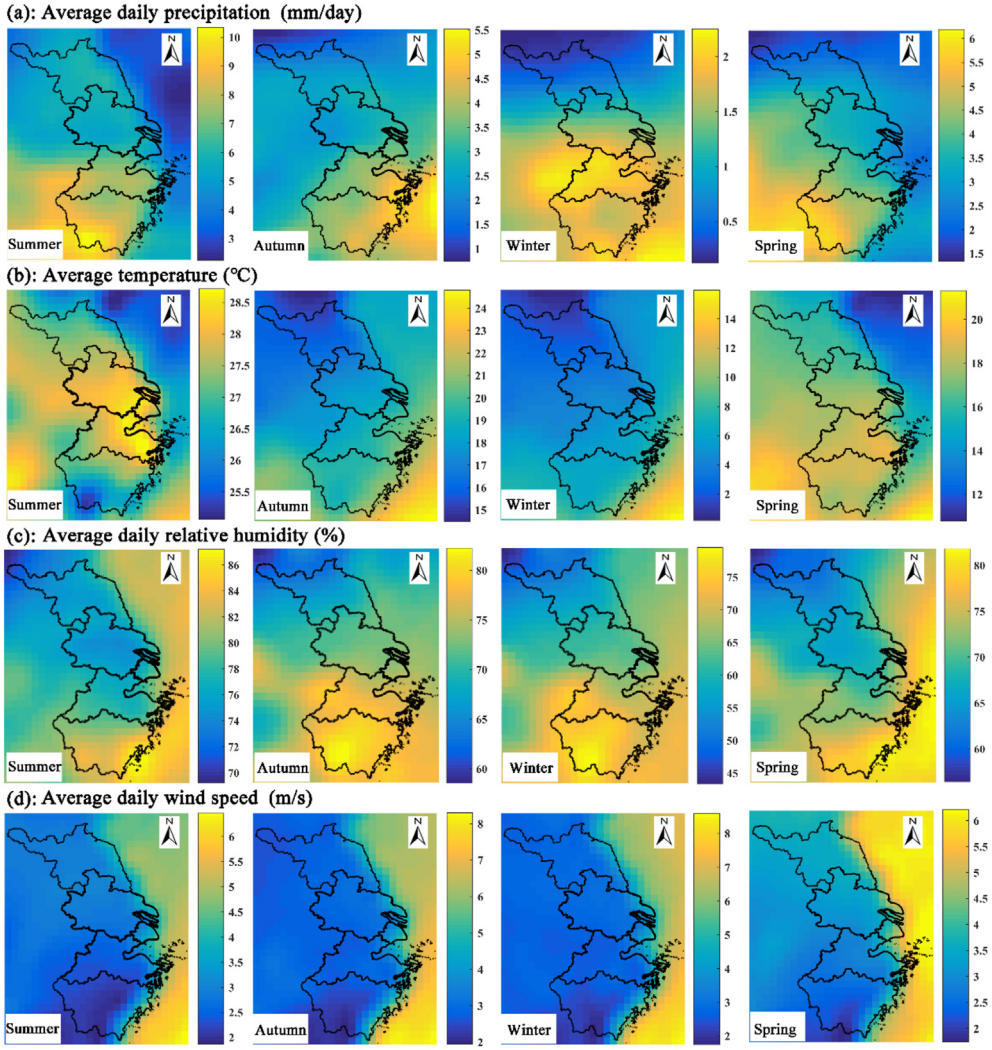

Fig. 2. (a) Average daily precipitation (mm/day), (b) average temperature (°C), (c) average daily relative humidity (%), and (d) average wind speed (m/s) in different seasons over the Yangtze River Delta.

3. Results and discussion

3.1. Characteristics of and long-term trend in atmospheric PAHs

3.1.1. Characteristics of atmospheric PAHs

From summer 2017 to spring 2018, the concentrations of the 16 studied PAHs in the YRD ranged from 13.00 to 88.71 ng/m^3 with an average concentration of 41.46 ± 15.57 ng/m^3. The average carcinogenic PAH concentration was 9.85 ± 5.47 ng/m^3, accounting for 23.76% of the total PAH concentration. The PAH concentration was significantly lower than that measured in Xi'an in 2012 (622 ng/m^3) (Wei et al., 2015), Beijing in 2015 (405 ng/m^3) (Cao et al., 2018), Dalian in 2016 (52.37 ng/m^3) (Wang et al., 2019) and other northern Chinese cities (Zhang et al., 2016). These patterns arose mainly because of the significant difference in energy consumption between northern and southern China. Large amounts of biomass and coal are burned, resulting in greater emissions of PAHs in northern China, especially in the heating season (Zhang et al., 2016). The PAH concentrations in this study were larger than those in some developed regions, such as the USA (Sun et al., 2006), Europe (Garrido et al., 2014), Japan (Hong et al., 2016), and South Korea (Choi et al., 2007). In terms of PAH composition, PHE and FLA contributed most, accounting for 30.84 and 13.13% of the total PAH concentrations, which is in line with previous studies (Ma et al., 2018). Fig. 3 shows the concentration of each PAH species in the YRD.

3.1.2. Long-term trend in atmospheric PAHs

To date, the level of pollution in the YRD region as a whole has been poorly understood. Most studies investigating the concentrations of PAHs focused on a few cities in the YRD, such as Nanjing (He et al., 2014) and Shanghai (Liu et al., 2018). To shed light on the historical trends in the YRD, we collected the reported atmospheric PAH concentrations in Nanjing (capital of Jiangsu), Hangzhou (capital of Zhejiang), and Shanghai (references are list in the Supplementary Materials). Because various analytical and sampling methods were used in these previous studies, the concentrations of the 16 PAHs could not be accurately compared. So the historical trend in BaP were compared instead, as it is also the only priority PAH regulated in the Chinese national air quality standard (Fig. 4).

The concentration of PAHs in all three cities have decreased significantly since 2001 (Shanghai: $R = 0.75$ $P < 0.05$; Nanjing: $R = 0.88$ $P < 0.01$; Hangzhou: $R = 0.99$ $P < 0.01$). This was likely caused by a combination of factors: First, with the improvement of living standards in the YRD, traditional household stoves were replaced by improved stoves, and the use of cleaner natural gas has increased annually (NBSC, 2018b). This has led to a rapid decline in PAH emissions from coal and biomass combustion, but this source nevertheless remains the largest PAH emitter in China (Shen et al., 2013). The industrial sector in the YRD is also continually employing technological innovations, and some heavy polluting industries, such as the primary aluminum industry, have been eliminated (Li et al., 2018). In addition, under the continuous pressure of severe haze, the Chinese government has recently introduced a series of pollution prevention measures and strict control of pollutant emissions (e.g., the Air Pollution Prevention and Control Action Plan). Strict policy control has also contributed to the reduction of atmospheric PAHs in the region (Li et al., 2016b).

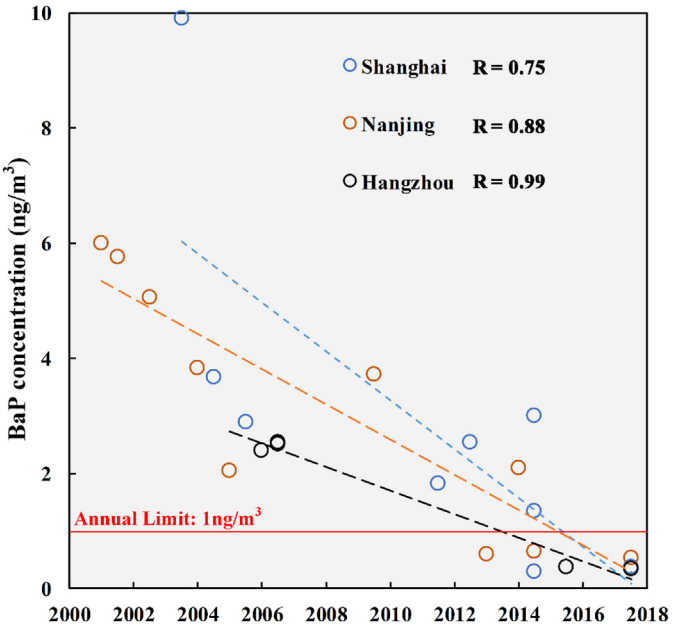

Fig. 4. Long-term trends in atmospheric BaP concentrations in Shanghai, Nanjing, and Hangzhou.

3.2. Spatio-temporal distribution of atmospheric PAHs

3.2.1. Spatial distribution of atmospheric PAHs

The atmospheric PAH concentrations in the YRD showed

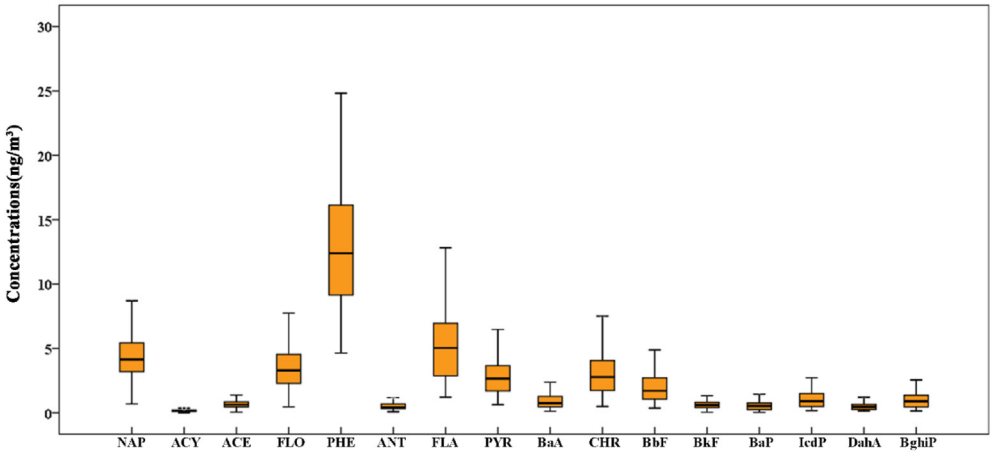

Fig. 3. Concentration of PAH species in the Yangtze River Delta.

pronounced spatial variation, where the high concentration areas were mainly located in Jiangsu (Fig. 5). The highest PAH concentration, with an annual average of 71.71 ng/m^3, was located in Zhenjiang. Zhenjiang has a large number of heavy industrial enterprises. The gross industrial output value of heavy industry in Zhenjiang accounts for 83.12% of its total industrial output value (ZSB, 2018), and heavy industrial enterprises emit more PAHs than other enterprises do. The lowest annual average PAH concentration (22.02 ng/m^3) was detected in the rural area of Tonglu, Hangzhou (site #23). Tonglu is a national forest county, surrounded by low hills and a good ecological environment. The area with the lowest PAH concentration (27.22 ng/m^3) among urban samples (site #27) was measured in Ningbo. As Ningbo is located on China's east coast, it receives relatively clean air from the ocean and has good atmospheric diffusion conditions compared with those of the other regions. This may be the main reason for the low concentration of PAHs in Ningbo. The PAH concentration in Shanghai (site #19) was also low. In addition to good meteorological conditions, Shanghai, as an international metropolis, has stricter air pollution control policies and regulations than other regions do (e.g., Shanghai Integrated Emission Standards for Air Pollutants and Shanghai Air Pollution Prevention and Control Regulations).

The annual average concentrations of the 16 measured PAHs in Jiangsu, Zhejiang, and Shanghai were 44.47 ± 11.37, 36.04 ± 9.39, and 36.62 ± 4.79 ng/m^3, respectively. The concentration of carcinogenic PAHs in the three regions were 11.71 ± 4.31, 7.32 ± 2.89, and 5.11 ± 1.04 ng/m^3, respectively (Table 1). The concentrations of the 16 PAHs in Jiangsu were 1.23 and 1.21 times higher than those in Zhejiang and Shanghai, while the concentrations of carcinogenic PAHs in Jiangsu were 1.60 and 2.29 times higher than those in Zhejiang and in Shanghai. These results not only show that the concentration of total PAHs in Jiangsu was high but also that carcinogenic PAHs accounted for a higher proportion of total PAHs in this region. There are three main reasons for these patterns: Firstly, Jiangsu is a large grain-producing province, and its rural non-commodity energy consumption (such as straw and firewood) is higher than that in Zhejiang and Shanghai (Cong et al., 2017). Secondly, Shandong, Hebei, and other regions in northern China have higher PAH emissions from coal and biomass combustion. These regions are close to Jiangsu, and this province is therefore more readily exposed to air masses from northern China (Zhang et al., 2016) (refer to Section 3.3.3). Comparing emission factors from different sources, coal and biomass combustion might emit more carcinogenic PAHs than other sources do (Shen et al., 2013). Furthermore, the industrial structure of different regions likely caused the higher concentrations of carcinogenic PAHs in Jiangsu. In 2016, the total industrial output value of heavy industry in Jiangsu was 2.29 and 5.06 times higher than that of Zhejiang and Shanghai, respectively. The contribution of the high energy consumption industry to the industrial output value in Jiangsu (24.25%) was also higher than that of Zhejiang (19.50%) and Shanghai (21.32%), and heavy industries emitted more industrial PAHs in Jiangsu than in the other two regions (Li et al., 2018).

Table 1
Average PAH concentration in Yangtze River Delta.

	Jiangsu		Zhejiang		Shanghai	
	Mean	STD	Mean	STD	Mean	STD
NAP	4.89	1.48	4.60	1.44	9.51	7.73
ACY	0.16	0.05	0.17	0.04	0.17	0.09
ACE	0.71	0.24	0.76	0.41	1.12	0.59
FLO	3.75	0.91	3.75	1.51	3.79	1.36
PHE	13.69	3.45	11.20	2.73	11.08	5.52
ANT	0.56	0.25	0.72	0.40	0.60	0.43
FLA	5.95	2.37	4.80	2.31	3.61	2.51
PYR	3.04	1.18	2.74	1.21	1.65	0.99
BaA	1.05	0.35	0.80	0.34	0.40	0.09
CHR	3.53	1.41	2.47	1.30	1.39	0.39
BbF	2.49	0.91	1.37	0.66	0.95	0.19
BkF	0.74	0.21	0.46	0.15	0.35	0.03
BaP	0.72	0.40	0.37	0.06	0.38	0.05
IcdP	1.35	0.48	0.76	0.26	0.63	0.14
DahA	0.57	0.24	0.42	0.04	0.39	0.05
BghiP	1.27	0.60	0.67	0.19	0.62	0.09
Carc-PAHs	11.71	4.31	7.32	2.89	5.11	1.04
16 PAHs	44.47	11.37	36.04	9.39	36.62	4.79

The total PAH concentrations in urban and rural areas in the YRD were 42.49 ± 15.67 and 37.91 ± 14.98 ng/m^3, respectively. The ratio between PAH concentrations in urban and rural areas was 1.12, which was close to the ratio in the North China Plain (1.23) (Liu et al., 2008) and Taiyuan (1.05) (Xia et al., 2013), but much lower than that in New Jersey, USA (7) (Gigliotti et al., 2005), Massachusetts, USA (46) (Allen et al., 1996), and Toronto, Canada (~3) (Motelay-Massei et al., 2005). Notably, the low efficiency of biomass and coal combustion in rural areas resulted in higher PAH emissions in northern China. However, in the YRD, the relatively balanced development between urban and rural areas was likely the main reason for the small difference in PAH concentrations

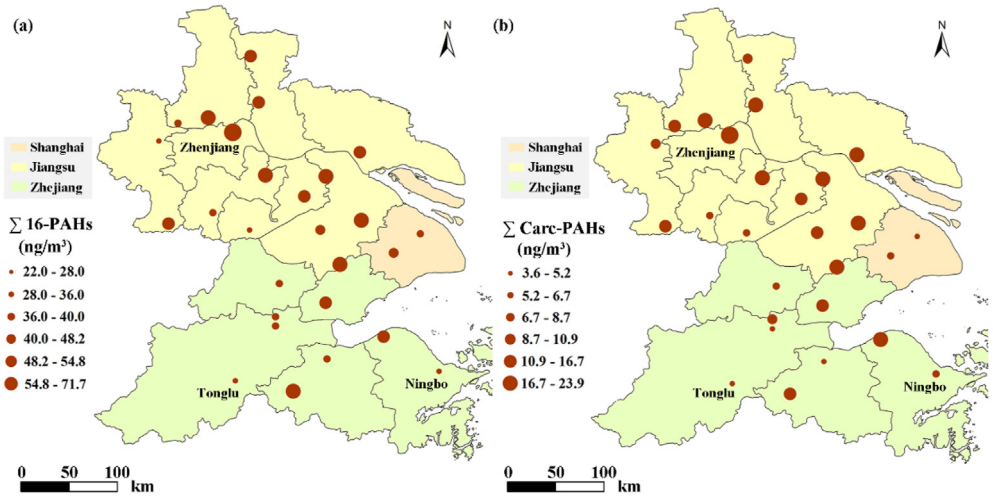

Fig. 5. Spatial distribution of PAH concentrations (ng/m^3) in China: (a) 16 studied PAHs and (b) carcinogenic PAHs.

between these areas (Long et al., 2009). The industrial and population density in some rural areas, such as Huaxi village, are similar to those in urban areas.

3.2.2. Seasonal variation in atmospheric PAH concentrations

In the YRD, the total PAH concentrations in the four seasons differed significantly ($P < 0.01$) (Fig. 6). It was highest in winter (52.21 ± 14.70 ng/m^3), followed by spring (43.07 ± 14.97 ng/m^3) and autumn (39.40 ± 12.45 ng/m^3), and it was lowest in summer (31.23 ± 12.88 ng/m^3). The concentration of carcinogenic PAHs in spring, summer, autumn, and winter were 9.17 ± 5.24, 6.24 ± 3.31, 11.27 ± 5.66, and 12.69 ± 5.33 ng/m^3, respectively. The trend of a higher concentration in winter and a lower concentration in summer was consistent with the results of previous studies (Liu et al., 2008).

The high PAH concentrations in winter were probably due to the contribution of outside sources. In winter, the prevailing wind direction in the YRD is northeast, which brings highly polluted air masses from northern China to the sampling sites (refer to section 3.3.3). And low temperatures and short sunshine periods are not conducive to the degradation of atmospheric PAHs (Tian et al., 2009). In summer, the Asian monsoon brings in clean air from the unstable rainy weather, where large amounts of PAHs in the atmosphere settle to the ground through wet deposition. The PAH concentration ratio in winter to summer in the YRD was 1.67 (Table S2), whereas the winter/summer ratios in northern China ranged between 2 and 13. In particular, the winter/summer ratios in Lanzhou, northern China, were 5–13 (Ma et al., 2018) and were mainly affected by the coal and biomass combustion used for heating in winter. The PAH winter/summer ratio in Jiangsu (1.76) was higher than that in Shanghai (1.46) and Zhejiang (1.46), which is likely because Jiangsu is located closer to northern China.

The PAH concentrations in most of the individual samples showed a similar trend, namely higher in winter and lower in summer. However, the PAH concentrations in some samples (sites #07, #10, #14) were highest in autumn, which was likely due to local/regional emission sources and hazy weather (Niu et al., 2017). $PM_{2.5}$ concentrations were often high on hazy days and could adsorb particulate PAHs. Particulate PAHs thus adsorbed by were found to have the highest concentrations in autumn in these three samples. We also found that the PAH concentrations in some samples (sites #18, #21, #24, and #25) were higher in summer than in spring and autumn, which might be due to the large amounts of low molecular weight PAHs evaporating from soil into the air during summer as a result of the high temperature (Wang et al., 2011). All of the four samplers were located in old residential areas, which may have higher pollution of soil PAHs than other areas as they would have accumulated for a longer period of time (Peng et al., 2011); therefore, more low molecular weight PAHs in the soil at the four sampling points may have evaporated into the air than at other sampling points. We also found that, during summer, the average PAHs ratio of two to three rings at the four

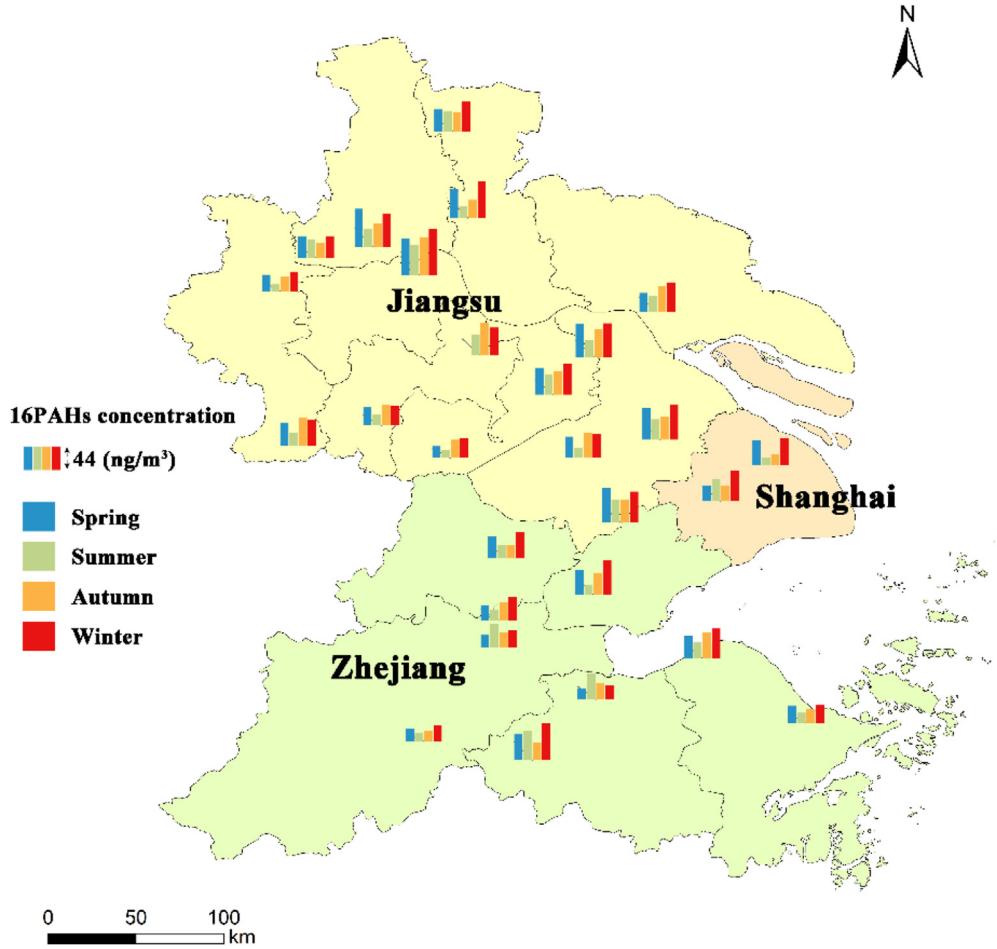

Fig. 6. Seasonal variation in the concentrations of the 16 measured PAHs in the Yangtze River Delta, China. The 44 ng/m^3 in the legend represent half of the maximum PAH concentrations in the YRD and serve as a reference when comparing the bars in the figure.

sampling sites (74.8%) was much higher than that at the other sites (55.7%).

3.3. Factors influencing atmospheric PAHs

3.3.1. Source identification

Three PCs were identified in this study, which explained 84.5% of the total variance in the dataset (Table S3). PC1 was heavily influenced by BaA, BbF, BkF, BaP, InP, DahA, and BghiP. According to previous studies (Han et al., 2009), BkF, IcdP, and BghiP are considered to be tracers of traffic source. PC2 was highly loaded with FLA, PYR, CHR, BbF, and PHE. Among these species, FLA and PYR have been used to fingerprint biomass combustion (Jenkins et al., 1996). Furthermore, PHE, FLA, BbF, and CHR have been reported to be the main components released during coal combustion (Chen et al., 2005) and can thus be used as markers for coal and biomass combustion. PC3 was highly loaded with low molecular weight PAHs, such as NAP, ACY, ACE, FLO, and ANT. Of these, NAP, ACY, and ACE have been reported to be the main components in the volatilization of crude oil and petroleum products (Yunker et al., 2002). In addition, FLO has been used as a tracer for coke oven sources of PAHs (Simcik et al., 1999). PC3 was highly loaded in summer but showed little seasonal variation. Therefore, the source indicated by this PC was a mixture of coke ovens and volatilization. After the PCA, we performed MLR analyses to identify the contributions of each source to PAH concentrations. The PCs were regressed against the concentrations of the total 16 PAHs for the four seasons.

During the sampling period, the average contribution of traffic, coal and biomass combustion, and coke ovens and volatilization were 52.83, 23.67, and 23.51%, respectively. Although emission factors of vehicles decreased with increasing implementation of staged emission standards, this positive development was offset by the sharp increase in vehicles on roads. In addition, the reduction of other sources, such as biomass burning, increased the contribution of traffic emissions. The high contribution of traffic was consistent with the results of other studies (Liu et al., 2018).

Coal and biomass combustion and traffic significantly differed with season (Fig. 7). The proportion of coal and biomass combustion was highest in winter (31.17%) and lowest in summer (7.67%). As the YRD is one of the most developed regions in China, unlike some regions in northern China (Zhang et al., 2016), coal and biomass combustion was relatively small. For example, the total domestic coal consumption in Shanghai, Jiangsu, and Zhejiang in 2017 was only 0.43 Mt, whereas it was 15.64 Mt in Hebei alone (NBSC, 2018b). However, we also found that the proportion of coal and biomass combustion to PAH concentrations in winter exceeded 30%. This was probably because the prevailing wind transported polluted air masses from northern China to the sampling sites (Fig. 8(d)). The proportional change in the traffic sources was mainly due to the seasonal differences in the amounts of coal and biomass combustion. Another reason may be that, during winter, some areas of the YRD and northern China have implemented traffic control measures to mitigate the heavy pollution, which reduced the emissions from traffic. Moreover, in summer, the traffic sources in southern China accounted for a high proportion (Li et al., 2006). The south-dominated wind transported air mass from southern China might be one reason for the contribution of traffic sources to PAHs concentrations exceeding 65% in YRD.

3.3.2. Impact of meteorological conditions

Total PAH concentration was significantly negatively correlated to precipitation and temperature throughout the year ($P < 0.01$) (Table 2). Precipitation removes both light and heavy molecular-weight PAHs (Li et al., 2016a), which explains its negative correlation with PAH concentrations. Total PAH concentrations were significantly correlated with precipitation in autumn and winter ($P < 0.05$). This was not the case in summer, when the average daily precipitation was high. The average cumulative precipitation in summer was 2091 mm, much higher than that in other seasons, which had an average cumulative precipitation of 769 mm. Higher precipitation washed out atmospheric PM and PAHs, which might have led to a poor reflection of the true correlation between precipitation and PAH concentrations. Higher temperatures not only increased the contribution of PAHs to the vapor phase but also caused greater PAH degradation, which is consistent with the results of previous studies (Yin and Xu, 2018). However, we found that the temperature was not significantly related to the PAH levels in summer and winter. The excessive rainfall in summer would weaken the effect of temperature on the level of PAHs. And in

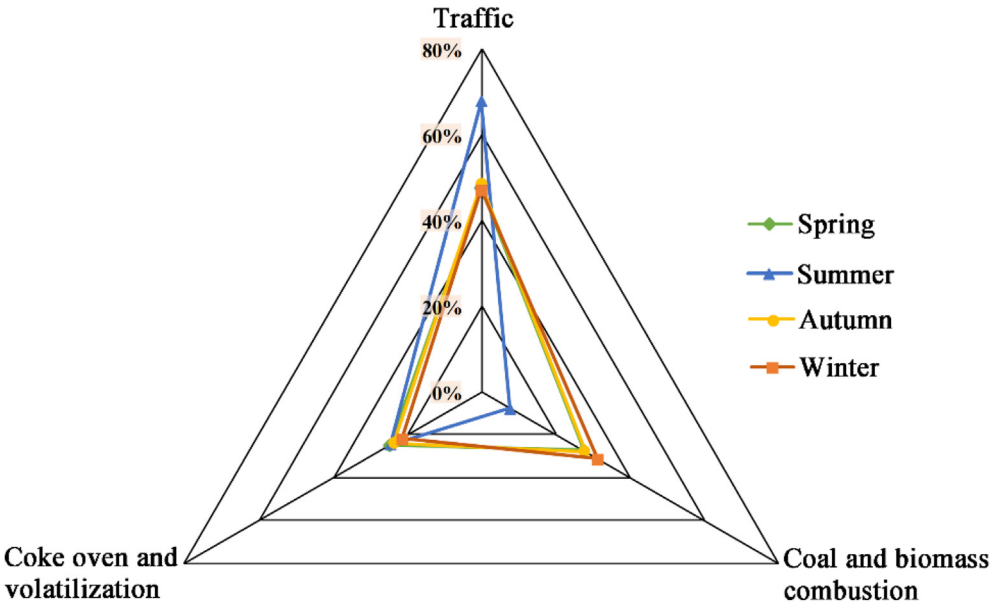

Fig. 7. Contribution of different sources to atmospheric polycyclic aromatic hydrocarbon (PAH) concentrations in different seasons.

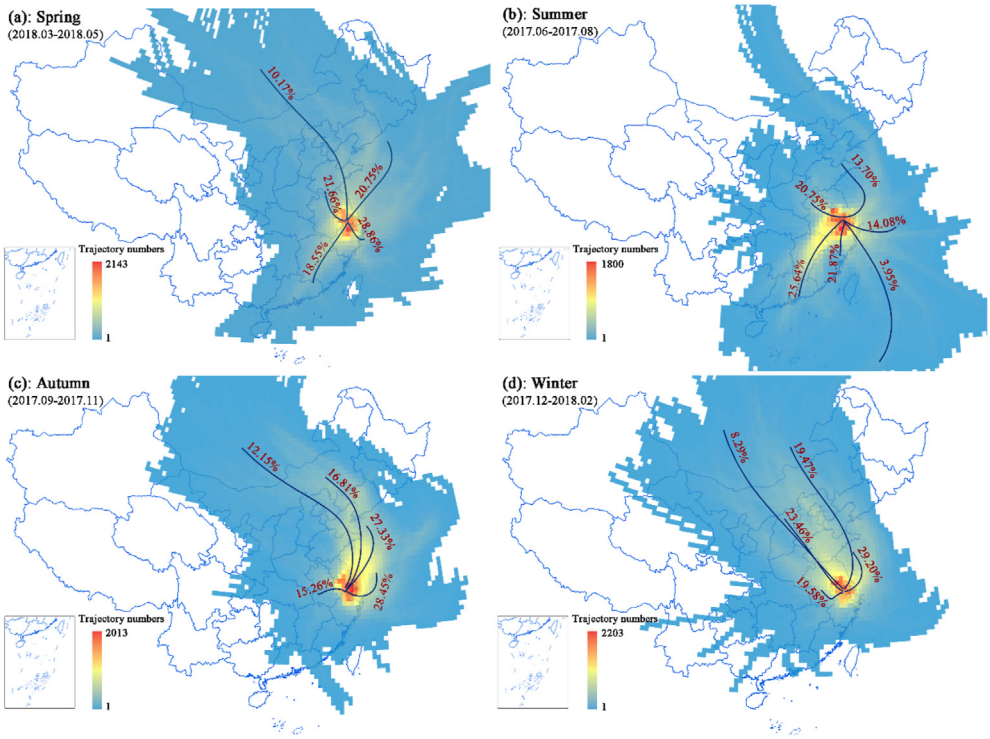

Fig. 8. Backward trajectory clusters and trajectory numbers in each 0.5° grid in the Yangtze River Delta, China.

Table 2
Correlation between total polycyclic aromatic hydrocarbon concentrations and precipitation, temperature, relative humidity, and wind speed.

	Correlation coefficients (r)			
	Precipitation	Temperature	Relative humidity	Wind speed
Whole year	−0.524**	−0.488**	−0.534**	−0.184
Spring	−0.339	−0.484*	−0.360	−0.249
Summer	0.023	0.082	−0.166	−0.208
Autumn	−0.413*	−0.409*	−0.387*	−0.151
Winter	−0.395*	−0.249	−0.345	−0.232

Note: * indicates significant correlation at 0.05 level, and ** indicates significant correlation at 0.01 level.

winter, the high PAH emission levels in YRD and large amounts of polluted air masses from northern China may lead to a weak correlation between temperature and the level of PAHs.

The relative humidity was also significantly negatively correlated with the concentration of PAHs throughout the year. However, the correlation in all seasons, excluding autumn, were not significant. Liu et al. (2018) suggested that relative humidity removes atmospheric PAHs, while some studies found that the level of PAHs is positively correlated (Hien et al., 2007) or weakly correlated (He et al., 2014) with the relative humidity. Therefore, the influence of relative humidity on PAHs is complex and requires further studies. Wind, as the main medium of pollutant transport, was negatively correlated with PAH concentrations, but the relationship was not significant. This was probably because we used the average wind speed of the whole quarter in the analysis, which might be too coarse a measure for detecting the effects of wind on PAH concentrations. Thus, we used the backward trajectory to analyze the influence of wind on PAH concentrations (Section 3.3.3).

3.3.3. Air mass backward trajectory

The backward trajectories in spring, summer, autumn, and winter were finally clustered into 5, 6, 5, and 5 according to total spatial variance (Fig. 8). The number of backward trajectories at the 0.5° grid was also calculated. We found that the seasonal difference in PAH concentrations was related to the source of air mass. For example, affected by the northwestern monsoon, the northwestern wind prevails in winter. More than 80% of the air mass came from Hebei, Shandong, Inner Mongolia, Liaoning, and other northern regions of China to the study sites. Highly polluted air masses (including large amounts of PAHs from coal and biomass combustion) from northern China entered the YRD in winter. In summer, due to the comprehensive influence of the southeastern and southwestern monsoon, 47.51% of the air masses come from Fujian, Guangdong, and other southern regions, and 18.03% from the sea. The probability of incoming air masses from northern China was thus greatly reduced (34.45%) during this season. In conclusion, PAHs in the YRD were significantly affected by external air masses, especially in winter.

4. Conclusion

The identification of the spatio-temporal distribution of atmospheric PAHs and the analysis of its influencing factors in the YRD are important for developing control strategies for the reduction of health risks. However, most studies only focused on the PAH concentrations in a few cities. Simultaneous studies on atmospheric PAHs at multi-sites across the YRD are rare. In this study, the concentrations of PAHs across the YRD were simultaneously monitored from June 2017 to May 2018. The spatio-temporal distribution and long-term trend of the PAHs concentrations were analyzed. Three PAH sources (traffic, coal and biomass combustion, and coke oven and volatilization) and their seasonal variations were identified by PCA-MLR. The correlations between the PAH concentrations and meteorological conditions in the YRD were clarified, and the potential PAH pollution source areas were analyzed using backward trajectory analysis. To the best of our knowledge, this is the first

comprehensive study reporting the spatio-temporal distribution and influencing factors of ambient PAHs throughout the YRD region.

We found that the average concentration of 16 PAHs was 41.46 ± 15.57 ng/m^3. Compared with the previously reported PAH data in the YRD, our results indicated a significant decrease in PAH concentrations, mainly as a result of the continuous reduction of emissions from various sources and strict policy control in recent years. The annual average total PAH concentrations in Jiangsu, Zhejiang, and Shanghai were 44.47 ± 11.37, 36.04 ± 9.39, and 36.62 ± 4.79 ng/m^3, respectively. Jiangsu not only had the highest total PAH concentrations but also the highest proportion of carcinogenic PAHs. We mainly ascribed this to the higher coal and biomass combustion in Jiangsu than that in Zhejiang and Shanghai as well as its proximity to northern China, from which polluted air masses originate. A relatively balanced development between urban and rural areas in the YRD caused the ratio between PAH concentrations in urban and rural areas to be relatively low (~1.12). The PAH concentrations in the YRD were highest in winter (52.21 ± 14.70 ng/m^3) and lowest in summer (31.23 ± 12.88 ng/m^3). The PAH concentrations in most of the individual samples showed a similar trend, namely higher in winter and lower in summer.

The average contributions of traffic, coal and biomass combustion, and coke oven and volatilization to the PAHs were 52.83, 23.67, and 23.51%, respectively. The contributions of coal and biomass combustion and traffic varied significantly with season, which might be due to the seasonal variations in coal and biomass combustion, traffic control measures for severely polluted air in winter, and south-dominated wind direction during summer. The total PAH concentrations and temperature, precipitation, and relative humidity were significantly negatively correlated ($P < 0.01$) throughout the year. Through the backward trajectory analysis, we found that over 80% of highly polluted air masses entered the YRD from northern China during winter, while only 34.5% entered the region during summer, which indicates that air mass transport is the main reason for the seasonal variations in the concentration of PAHs in the YRD.

The paper provided several suggestions for controlling atmospheric PAHs in China. First, more strict controls of coal and biomass combustion in the residential sector should be implemented in the North China Plain and other northern regions of China, and the use of clean energy in these areas should be promoted, particularly during the heating season. Residential coal/biomass-burning cooking stoves should be replaced with improved stoves in rural households as soon as possible. These measures are the most important as the proportion of PAH emissions from the residential sector is the largest in China (Shen et al., 2013). Measures promoting clean fuels in the residential sector are currently being implemented in some northern regions, such as Beijing-Tianjin-Hebei, and energy consumption in many households has been switched from coal to electricity and natural gas (Zhang et al., 2019b). Second, regarding the relatively high proportion of PAHs contributed by traffic, the fuel quality of vehicles must be improved further. Vehicles that fail to meet the emissions standards should be phased out, and the proportion of gas/electric vehicles should be increased. Stricter traffic control measures, particularly for old and "yellow-label" vehicles, should be implemented. Lastly, it is necessary to strengthen the joint prevention and control of PAH pollution among various regions. To reduce the pollution by PAHs in a certain region, both local and regional sources should be comprehensively considered. For example, the PAH pollution in our study area was significantly affected by air masses from northern China.

Declaration of competing interest

The authors declare that they have no known competing financial interests or personal relationships that could have appeared to influence the work reported in this paper.

CRediT authorship contribution statement

Baojie Li: Conceptualization, Investigation, Methodology, Writing - original draft, Writing - review & editing. **Shenglu Zhou:** Conceptualization, Supervision, Resources, Writing - review & editing. **Teng Wang:** Methodology, Data curation. **Yujie Zhou:** Investigation. **Liang Ge:** Investigation. **Hong Liao:** Conceptualization, Supervision, Writing - review & editing.

Acknowledgements

We thank the anonymous reviewers for their valuable and constructive comments. This work was supported by the National Natural Science Foundation of China [grant numbers 41771243, 41671085], the Startup Foundation for Introducing Talent of NUIST (2020r016), and the Natural Science Foundation of the Jiangsu Higher Education Institutions of China (18KJB170004).

Appendix A. Supplementary data

Supplementary data related to this article can be found at https://doi.org/10.1016/j.jclepro.2020.122049.

References

Allen, J.O., Dookeran, N.M., Smith, K.A., Sarofim, A.F., Taghizadeh, K., Lafleur, A.L., 1996. Measurement of polycyclic aromatic hydrocarbons associated with size-segregated atmospheric aerosols in Massachusetts. Environ. Sci. Technol. 30 (3), 1023–1031.

Andersson, J.T., Achten, C., 2015. Time to say goodbye to the 16 EPA PAHs? Toward an up-to-date use of PACs for environmental purposes. Polycycl. Aromat. Comp. 35 (2–4), 330–354.

Cao, R., Zhang, H., Geng, N., Fu, Q., Teng, M., Zou, L., Gao, Y., Chen, J., 2018. Diurnal variations of atmospheric polycyclic aromatic hydrocarbons (PAHs) during three sequent winter haze episodes in Beijing, China. Sci. Total Environ. 625, 1486–1493.

Chang, K.-F., Fang, G.-C., Chen, J.-C., Wu, Y.-S., 2006. Atmospheric polycyclic aromatic hydrocarbons (PAHs) in Asia: a review from 1999 to 2004. Environ. Pollut. 142 (3), 388–396.

Chen, Y., Sheng, G., Bi, X., Feng, Y., Mai, B., Fu, J., 2005. Emission factors for carbonaceous particles and polycyclic aromatic hydrocarbons from residential coal combustion in China. Environ. Sci. Technol. 39 (6), 1861–1867.

Choi, S.D., Baek, S.Y., Chang, Y.S., 2007. Influence of a large steel complex on the spatial distribution of volatile polycyclic aromatic hydrocarbons (PAHs) determined by passive air sampling using membrane-enclosed copolymer (MECOP). Atmos. Environ. 41 (29), 6255–6264.

Cong, H., Zhao, L., Wang, J., Yao, Z., 2017. Current situation and development demand analysis of rural energy in China. Trans. Chin. Soc. Agric. Eng. 33 (17), 224–231.

ECMWF, 2009. ERA-interim Project. Research Data Archive at the National Center for Atmospheric Research, Computational and Information Systems Laboratory, Boulder, CO.

Garrido, A., Jiménez-Guerrero, P., Ratola, N., 2014. Levels, trends and health concerns of atmospheric PAHs in Europe. Atmos. Environ. 99, 474–484.

Gigliotti, C.L., Totten, L.A., Offenberg, J.H., Dachs, J., Reinfelder, J.R., Nelson, E.D., Glenn IV, T.R., Eisenreich, S.J., 2005. Atmospheric concentrations and deposition of polycyclic aromatic hydrocarbons to the Mid-Atlantic East Coast Region. Environ. Sci. Technol. 39 (15), 5550–5559.

Han, B., Bai, Z., Guo, G., Wang, F., Li, F., Liu, Q., Ji, Y., Li, X., Hu, Y., 2009. Characterization of PM10 fraction of road dust for polycyclic aromatic hydrocarbons (PAHs) from Anshan, China. J. Hazard Mater. 170 (2), 934–940.

He, J., Fan, S., Meng, Q., Sun, Y., Zhang, J., Zu, F., 2014. Polycyclic aromatic hydrocarbons (PAHs) associated with fine particulate matters in Nanjing, China: distributions, sources and meteorological influences. Atmos. Environ. 89, 207–215.

Hien, T.T., Nam, P.P., Yasuhiro, S., Takayuki, K., Norimichi, T., Hiroshi, B., 2007. Comparison of particle-phase polycyclic aromatic hydrocarbons and their variability causes in the ambient air in Ho Chi Minh City, Vietnam and in Osaka, Japan, during 2005–2006. Sci. Total Environ. 382 (1), 70–81.

Hong, W., Jia, H., Ma, W.L., Sinha, R.K., Moon, H.B., Nakata, H., Minh, N.H., Chi, K.H., Li, W.L., Kannan, K., 2016. Distribution, fate, inhalation exposure and lung cancer risk of atmospheric polycyclic aromatic hydrocarbons in some Asian countries. Environ. Sci. Technol. 50 (13), 7163–7174.
Jenkins, B.M., Jones, A.D., Turn, S.Q., Williams, R.B., 1996. Emission factors for polycyclic aromatic hydrocarbons from biomass burning. Environ. Sci. Technol. 30 (8), 2462–2469.
Keith, L.H., 2015. The source of U.S. EPA's sixteen PAH priority pollutants. Polycycl. Aromat. Comp. 35 (2–4), 147–160.
Lang, C., Tao, S., Liu, W., Zhang, Y., Simonich, S., 2008. Atmospheric transport and outflow of polycyclic aromatic hydrocarbons from China. Environ. Sci. Technol. 42 (14), 5196–5201.
Larsen, R.K., Baker, J.E., 2003. Source apportionment of polycyclic aromatic hydrocarbons in the urban Atmosphere: A comparison of three methods. Environ. Sci. Technol. 37 (9), 1873–1881.
Li, B., Zhou, S., Wang, T., Sui, X., Jia, Z., Li, Y., Wang, J., Wu, S., 2018. An improved gridded polycyclic aromatic hydrocarbon emission inventory for the lower reaches of the Yangtze River Delta region from 2001 to 2015 using satellite data. J. Hazard Mater. 360, 329–339.
Li, J., Zhang, G., Li, X., Qi, S., Liu, G., Peng, X., 2006. Source seasonality of polycyclic aromatic hydrocarbons (PAHs) in a subtropical city, Guangzhou, South China. Sci. Total Environ. 355 (1), 145–155.
Li, K., Jacob, D.J., Liao, H., Zhu, J., Shah, V., Shen, L., Bates, K.H., Zhang, Q., Zhai, S., 2019. A two-pollutant strategy for improving ozone and particulate air quality in China. Nat. Geosci. 12 (11), 906–910.
Li, P.-h., Wang, Y., Li, Y.-h., Wai, K.-m., Li, H.-l., Tong, L., 2016a. Gas-particle partitioning and precipitation scavenging of polycyclic aromatic hydrocarbons (PAHs) in the free troposphere in southern China. Atmos. Environ. 128, 165–174.
Li, X., Kong, S., Yin, Y., Li, L., Yuan, L., Li, Q., Xiao, H., Chen, K., 2016b. Polycyclic aromatic hydrocarbons (PAHs) in atmospheric PM2.5 around 2013 Asian Youth Games period in Nanjing. Atmos. Res. 174–175, 85–96.
Lin, Y., Ma, Y., Qiu, X., Li, R., Fang, Y., Wang, J., Zhu, Y., Hu, D., 2015. Sources, transformation, and health implications of PAHs and their nitrated, hydroxylated, and oxygenated derivatives in PM2.5 in Beijing. J. Geophys. Res.: Atmos. 120 (14), 7219–7228.
Liu, S., Tao, S., Liu, W., Dou, H., Liu, Y., Zhao, J., Little, M.G., Tian, Z., Wang, J., Wang, L., 2008. Seasonal and spatial occurrence and distribution of atmospheric polycyclic aromatic hydrocarbons (PAHs) in rural and urban areas of the North Chinese Plain. Environ. Pollut. 156 (3), 651–656.
Liu, Y., Yan, C., Ding, X., Wang, X., Fu, Q., Zhao, Q., Zhang, Y., Duan, Y., Qiu, X., Zheng, M., 2017. Sources and spatial distribution of particulate polycyclic aromatic hydrocarbons in Shanghai, China. Sci. Total Environ. 584–585, 307–317.
Liu, Y., Yu, Y., Liu, M., Lu, M., Ge, R., Li, S., Liu, X., Dong, W., Qadeer, A., 2018. Characterization and source identification of PM2.5-bound polycyclic aromatic hydrocarbons (PAHs) in different seasons from Shanghai, China. Sci. Total Environ. 644, 725–735.
Long, H., Liu, Y., Wu, X., Dong, G., 2009. Spatio-temporal dynamic patterns of farmland and rural settlements in Su–Xi–Chang region: implications for building a new countryside in coastal China. Land Use Pol. 26 (2), 322–333.
Ma, W.-L., Liu, L.-Y., Jia, H.-L., Yang, M., Li, Y.-F., 2018. PAHs in Chinese atmosphere Part I: concentration, source and temperature dependence. Atmos. Environ. 173, 330–337.
Ma, Y., Cheng, Y., Qiu, X., Lin, Y., Cao, J., Hu, D., 2016. A quantitative assessment of source contributions to fine particulate matter (PM2.5)-bound polycyclic aromatic hydrocarbons (PAHs) and their nitrated and hydroxylated derivatives in Hong Kong. Environ. Pollut. 219, 742–749.
Motelay-Massei, A., Harner, T., Shoeib, M., Diamond, M., Stern, G., Rosenberg, B., 2005. Using passive air samplers to assess Urban–Rural trends for persistent organic pollutants and polycyclic aromatic hydrocarbons. 2. Seasonal trends for PAHs, PCBs, and organochlorine pesticides. Environ. Sci. Technol. 39 (15), 5763–5773.
NBSC (National Bureau of Statistics of China), 2018a. China Statistical Yearbook 2017. China Statistics Press, Beijing, China.
NBSC (National Bureau of Statistics of China), 2018b. China Energy Statistical Yearbook 2017. China Statistics Press, Beijing, China.
Neroda, A.S., Goncharova, A.A., Mishukov, V.F., 2020. PAHs in the atmospheric aerosols and seawater in the North–West Pacific ocean and sea of Japan. Atmos. Environ. 222, 117117.
Niu, S., Dong, L., Zhang, L., Zhu, C., Hai, R., Huang, Y., 2017. Temporal and spatial distribution, sources, and potential health risks of ambient polycyclic aromatic hydrocarbons in the Yangtze River Delta (YRD) of eastern China. Chemosphere 172, 72–79.
Peng, C., Chen, W., Liao, X., Wang, M., Ouyang, Z., Jiao, W., Bai, Y., 2011. Polycyclic aromatic hydrocarbons in urban soils of Beijing: status, sources, distribution and potential risk. Environ. Pollut. 159 (3), 802–808.
Shen, H., Huang, Y., Wang, R., Zhu, D., Li, W., Shen, G., Wang, B., Zhang, Y., Chen, Y., Lu, Y., Chen, H., Li, T., Sun, K., Li, B., Liu, W., Liu, J., Tao, S., 2013. Global atmospheric emissions of polycyclic aromatic hydrocarbons from 1960 to 2008 and future predictions. Environ. Sci. Technol. 47 (12), 6415–6424.
Shen, R., Liu, Z., Chen, X., Wang, Y., Wang, L., Liu, Y., Li, X., 2019. Atmospheric levels, variations, sources and health risk of PM2.5-bound polycyclic aromatic hydrocarbons during winter over the North China Plain. Sci. Total Environ. 655, 581–590.
Simcik, M.F., Eisenreich, S.J., Lioy, P.J., 1999. Source apportionment and source/sink relationships of PAHs in the coastal atmosphere of Chicago and Lake Michigan. Atmos. Environ. 33 (30), 5071–5079.
Sun, P., Blanchard, P., Brice, K.A., Hites, R.A., 2006. Trends in polycyclic aromatic hydrocarbon concentrations in the great lakes atmosphere. Environ. Sci. Technol. 40 (20), 6221–6227.
Tan, J.-H., Bi, X.-H., Duan, J.-C., Rahn, K.A., Sheng, G.-Y., Fu, J.-M., 2006. Seasonal variation of particulate polycyclic aromatic hydrocarbons associated with PM10 in Guangzhou, China. Atmos. Res. 80 (4), 250–262.
Tian, F., Chen, J., Qiao, X., Wang, Z., Yang, P., Wang, D., Ge, L., 2009. Sources and seasonal variation of atmospheric polycyclic aromatic hydrocarbons in Dalian, China: factor analysis with non-negative constraints combined with local source fingerprints. Atmos. Environ. 43 (17), 2747–2753.
Wang, W., Simonich, S., Giri, B., Chang, Y., Zhang, Y., Jia, Y., Tao, S., Wang, R., Wang, B., Li, W., Cao, J., Lu, X., 2011. Atmospheric concentrations and air–soil gas exchange of polycyclic aromatic hydrocarbons (PAHs) in remote, rural village and urban areas of Beijing–Tianjin region, North China. Sci. Total Environ. 409 (15), 2942–2950.
Wang, Y., Zhang, Q., Zhang, Y., Zhao, H., Tan, F., Wu, X., Chen, J., 2019. Source apportionment of polycyclic aromatic hydrocarbons (PAHs) in the air of Dalian, China: correlations with six criteria air pollutants and meteorological conditions. Chemosphere 216, 516–523.
Wei, C., Han, Y., Bandowe, B.A.M., Cao, J., Huang, R.-J., Ni, H., Tian, J., Wilcke, W., 2015. Occurrence, gas/particle partitioning and carcinogenic risk of polycyclic aromatic hydrocarbons and their oxygen and nitrogen containing derivatives in Xi'an, central China. Sci. Total Environ. 505, 814–822.
Xia, Z., Duan, X., Tao, S., Qiu, W., Liu, D., Wang, Y., Wei, S., Wang, B., Jiang, Q., Lu, B., Song, Y., Hu, X., 2013. Pollution level, inhalation exposure and lung cancer risk of ambient atmospheric polycyclic aromatic hydrocarbons (PAHs) in Taiyuan, China. Environ. Pollut. 173, 150–156.
Xu, Y., Shen, H., Yun, X., Gao, F., Chen, Y., Li, B., Liu, J., Ma, J., Wang, X., Liu, X., Tian, C., Xing, B., Tao, S., 2018. Health effects of banning beehive coke ovens and implementation of the ban in China. Proc. Natl. Acad. Sci. Unit. States Am. 115 (11), 2693.
Yan, Y., He, Q., Guo, L., Li, H., Zhang, H., Shao, M., Wang, Y., 2017. Source apportionment and toxicity of atmospheric polycyclic aromatic hydrocarbons by PMF: quantifying the influence of coal usage in Taiyuan, China. Atmos. Res. 193, 50–59.
Yin, H., Xu, L., 2018. Comparative study of PM10/PM2.5-bound PAHs in downtown Beijing, China: concentrations, sources, and health risks. J. Clean. Prod. 177, 674–683.
Yunker, M.B., Macdonald, R.W., Vingarzan, R., Mitchell, R.H., Goyette, D., Sylvestre, S., 2002. PAHs in the Fraser River basin: a critical appraisal of PAH ratios as indicators of PAH source and composition. Org. Geochem. 33 (4), 489–515.
Zhang, J., Li, R., Zhang, X., Bai, Y., Cao, P., Hua, P., 2019a. Vehicular contribution of PAHs in size dependent road dust: a source apportionment by PCA-MLR, PMF, and Unmix receptor models. Sci. Total Environ. 649, 1314–1322.
Zhang, Q., Zheng, Y., Tong, D., Shao, M., Wang, S., Zhang, Y., Xu, X., Wang, J., He, H., Liu, W., 2019b. Drivers of improved PM2. 5 air quality in China from 2013 to 2017. Proc. Natl. Acad. Sci. Unit. States Am. 116 (49), 24463–24469.
Zhang, Y., Lin, Y., Cai, J., Liu, Y., Hong, L., Qin, M., Zhao, Y., Ma, J., Wang, X., Zhu, T., Qiu, X., Zheng, M., 2016. Atmospheric PAHs in north China: spatial distribution and sources. Sci. Total Environ. 565, 994–1000.
Zheng, J., Jiang, P., Qiao, W., Zhu, Y., Kennedy, E., 2016. Analysis of air pollution reduction and climate change mitigation in the industry sector of Yangtze River Delta in China. J. Clean. Prod. 114, 314–322.
ZSB (Zhenjiang Statistical Bureau), 2018. Statistical Yearbook of Zhenjiang 2017. China Statistics Press, Beijing, China.